

## REPORT DOCUMENTATION PAGE

Form Approved OMB NO. 0704-0188

The public reporting burden for this collection of information is estimated to average 1 hour per response, including the time for reviewing instructions, searching existing data sources, gathering and maintaining the data needed, and completing and reviewing the collection of information. Send comments regarding this burden estimate or any other aspect of this collection of information, including suggestions for reducing this burden, to Washington Headquarters Services, Directorate for Information Operations and Reports, 1215 Jefferson Davis Highway, Suite 1204, Arlington VA, 22202-4302. Respondents should be aware that notwithstanding any other provision of law, no person shall be subject to any penalty for failing to comply with a collection of information if it does not display a currently valid OMB control number.

PLEASE DO NOT RETURN YOUR FORM TO THE ABOVE ADDRESS.

1. REPORT DATE (DD-MM-YYYY)	2. REPORT TYPE	3. DATES COVERED (From - To)	
	New Reprint	-	
4. TITLE AND SUBTITLE  Ex Situ Thermal Cycle Annealing of Molecular Beam Epitaxy Grown HgCdTe/Si Layers		5a. CONTRACT NUMBER  W911NF-07-2-0055	5b. GRANT NUMBER
		5c. PROGRAM ELEMENT NUMBER  611102	5d. PROJECT NUMBER
6. AUTHORS  S. Farrell, G. Brill, Y. Chen, P. S. Wijewarnasuriya, Mulpuri V. Rao, N. Dhar, K. Harris		5e. TASK NUMBER	5f. WORK UNIT NUMBER
7. PERFORMING ORGANIZATION NAMES AND ADDRESSES  George Mason University Office of Sponsored Programs George Mason University Fairfax, VA 22030 -4422		8. PERFORMING ORGANIZATION REPORT NUMBER	
9. SPONSORING/MONITORING AGENCY NAME(S) AND ADDRESS(ES)  U.S. Army Research Office P.O. Box 12211 Research Triangle Park, NC 27709-2211		10. SPONSOR/MONITOR'S ACRONYM(S) ARO  11. SPONSOR/MONITOR'S REPORT NUMBER(S) 52589-EL.2	
12. DISTRIBUTION AVAILABILITY STATEMENT  Approved for public release; distribution is unlimited.			
13. SUPPLEMENTARY NOTES  The views, opinions and/or findings contained in this report are those of the author(s) and should not be construed as an official Department of the Army position, policy or decision, unless so designated by other documentation.			
14. ABSTRACT  We present the results of ex situ thermal cycle annealing (TCA) of molecular beam epitaxy grown mercury cadmium telluride (HgCdTe) on Cd(Se)Te/ Si(211) composite substrates. We examined the variation in the etch pit density (EPD) and overall crystalline quality with respect to annealing temperature, number of annealing cycles, total annealing time, pre-annealed EPD/crystal quality, buffer layer quality, and buffer layer lattice constant. Using TCA we observed an order of magnitude reduction in the dislocation density of the HgCdTe layers and a			
15. SUBJECT TERMS  Mercury cadmium telluride (HgCdTe), thermal cycle annealing, etch pit density (EPD), dislocations, molecular beam epitaxy (MBE), silicon (Si), composite substrates			
16. SECURITY CLASSIFICATION OF:  a. REPORT UU		17. LIMITATION OF ABSTRACT  b. ABSTRACT UU c. THIS PAGE UU	15. NUMBER OF PAGES  19a. NAME OF RESPONSIBLE PERSON Rao Mulpuri 19b. TELEPHONE NUMBER 703-993-1612

## Report Title

Ex Situ Thermal Cycle Annealing of Molecular Beam Epitaxy Grown HgCdTe/Si Layers

## ABSTRACT

We present the results of ex situ thermal cycle annealing (TCA) of molecular beam epitaxy grown mercury cadmium telluride (HgCdTe) on Cd(Se)Te/ Si(211) composite substrates. We examined the variation in the etch pit density (EPD) and overall crystalline quality with respect to annealing temperature, number of annealing cycles, total annealing time, pre-annealed EPD/crystal quality, buffer layer quality, and buffer layer lattice constant. Using TCA we observed an order of magnitude reduction in the dislocation density of the HgCdTe layers and a corresponding decrease in x-ray full width at half maximum, when the as-grown layer EPD was on the order of  $10^7 \text{ cm}^{-2}$ . Among all the parameters studied, the one with the greatest influence on reducing EPD was the number of annealing cycles. We also noticed a saturation point where the HgCdTe/Si EPD did not decrease below  $10^6 \text{ cm}^{-2}$ , regardless of further TCA treatment or the as-grown EPD value.

---

**REPORT DOCUMENTATION PAGE (SF298)**  
**(Continuation Sheet)**

---

Continuation for Block 13

ARO Report Number 52589.2-EL  
Ex Situ Thermal Cycle Annealing of Molecular B ...

Block 13: Supplementary Note

© 2009 . Published in Journal of Electronic Materials, Vol. Ed. 0 39, (1) (2009), (1). DoD Components reserve a royalty-free, nonexclusive and irrevocable right to reproduce, publish, or otherwise use the work for Federal purposes, and to authroize others to do so (DODGARS §32.36). The views, opinions and/or findings contained in this report are those of the author(s) and should not be construed as an official Department of the Army position, policy or decision, unless so designated by other documentation.

Approved for public release; distribution is unlimited.

# Ex Situ Thermal Cycle Annealing of Molecular Beam Epitaxy Grown HgCdTe/Si Layers

S. FARRELL,<sup>1</sup> G. BRILL,<sup>2</sup> Y. CHEN,<sup>2</sup> P.S. WIJEWARNASURIYA,<sup>2,5</sup>  
MULPURI V. RAO,<sup>1</sup> N. DHAR,<sup>3</sup> and K. HARRIS<sup>4</sup>

1.—Department of Electrical and Computer Engineering, George Mason University, Fairfax, VA 22030-4444, USA. 2.—U.S. Army Research Laboratory, Sensors and Electron Devices Directorate, 2800 Powder Mill Road, Adelphi, MD 20783, USA. 3.—DARPA, Microsystems Technology Office (MTO), 3701 North Fairfax Drive, Arlington, VA 22203-1714, USA. 4.—Penn State Electro-Optics Center, 222 Northpointe Blvd., Freeport, PA 16229, USA. 5.—e-mail: priyalal.wijewarnasuriya@us.army.mil

We present the results of *ex situ* thermal cycle annealing (TCA) of molecular beam epitaxy grown mercury cadmium telluride (HgCdTe) on Cd(Se)Te/Si(211) composite substrates. We examined the variation in the etch pit density (EPD) and overall crystalline quality with respect to annealing temperature, number of annealing cycles, total annealing time, pre-annealed EPD/crystal quality, buffer layer quality, and buffer layer lattice constant. Using TCA we observed an order of magnitude reduction in the dislocation density of the HgCdTe layers and a corresponding decrease in x-ray full width at half maximum, when the as-grown layer EPD was on the order of  $1 \times 10^7 \text{ cm}^{-2}$ . Among all the parameters studied, the one with the greatest influence on reducing EPD was the number of annealing cycles. We also noticed a saturation point where the HgCdTe/Si EPD did not decrease below  $\sim 1 \times 10^6 \text{ cm}^{-2}$ , regardless of further TCA treatment or the as-grown EPD value.

**Key words:** Mercury cadmium telluride (HgCdTe), thermal cycle annealing, etch pit density (EPD), dislocations, molecular beam epitaxy (MBE), silicon (Si), composite substrates

## INTRODUCTION

HgCdTe on Si technologies are effective means for producing short wavelength infrared (SWIR) and medium wavelength infrared (MWIR) focal plane arrays.<sup>1–3</sup> However, there remains a problem with defects causing shorter lifetimes and lowering the mobility of minority carriers, and large dark currents in long wavelength infrared (LWIR) detectors.<sup>4,5</sup> Current growth methods of HgCdTe/CdTe/Si result in a dislocation density of mid- to high  $10^6 \text{ cm}^{-2}$ , which is relatively high in comparison with the HgCdTe growth on lattice-matched bulk CdZnTe substrates.

Recent work<sup>6</sup> on CdTe/Si has shown that *in situ* thermal cycle annealing (TCA), where annealing is performed intermittently during the growth process itself, is an effective means to reduce etch pit density (EPD) and improve overall crystal quality. Subjecting CdTe/Si layers to multiple cycle *in situ* annealing can result in a reduction of EPD up to a saturation point of mid- $10^5 \text{ cm}^{-2}$ . Similar *in situ* cycle annealing on HgCdTe/GaAs at 350–490°C has resulted in an EPD of  $2\text{--}4 \times 10^6 \text{ cm}^{-2}$  from the base line growth value of  $9\text{--}20 \times 10^6 \text{ cm}^{-2}$ .<sup>7</sup> Owing to the high mercury over-pressure needed to maintain the surface morphologies and composition of HgCdTe, a cap layer of ZnTe or ZnSe was used in those annealing experiments. Shin et al.<sup>8</sup> reported an EPD reduction of HgCdTe/GaAs using *ex situ* TCA, where annealing was performed outside the growth system and the epilayer was not specially capped

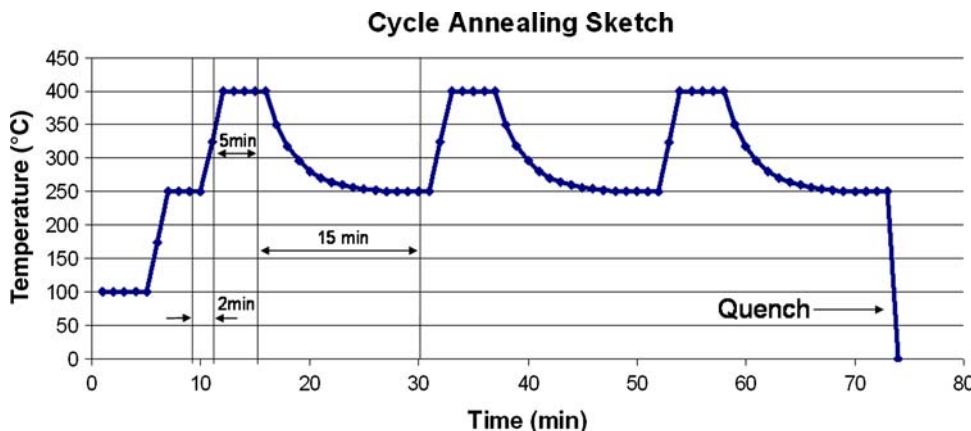


Fig. 1. Temperature versus time schematic of a three-cycle annealing process for a maximum annealing temperature of 400°C.

and was exposed to a heavy mercury over-pressure. This method of cycle annealing was effective in reducing EPD in HgCdTe/GaAs to mid- $10^5$  cm $^{-2}$ .<sup>8,9</sup>

In this paper we present our results from a detailed study of *ex situ* cycle annealing of HgCdTe/CdTe/Si. In our study we examined the variation in EPD and the overall crystalline quality with respect to annealing temperature, number of annealing cycles, total annealing time, pre-annealed EPD/crystal quality, Cd composition, buffer layer quality, and buffer layer lattice constant. For comparison, we also examined the effects of TCA on the HgCdTe layer grown on lattice-matched ( $x \approx 0.04$ ) Cd $_{1-x}$ Se $_x$ Te/Si substrates and on bulk lattice-matched ( $x \approx 0.04$ ) Cd $_{1-x}$ Zn $_x$ Te substrates.

## EXPERIMENT

The samples used in this study were grown by molecular beam epitaxy (MBE) on composite CdTe/Si substrates, except where noted. Details of the CdTe/Si growth process have been described elsewhere.<sup>6,10</sup> In brief, CdTe was nucleated on 3-in. nominal substrates using arsenic passivation of the Si surface followed by the growth of a thin ZnTe buffer layer. The subsequent CdTe layer was grown to a thickness of approximately 9  $\mu$ m. One HgCdTe layer was grown on a lattice-matched CdSeTe/Si composite substrate, while another HgCdTe layer used in this study was grown on a bulk CdZnTe substrate for comparison. The HgCdTe was grown at  $\sim 185^\circ\text{C}$ , with a growth rate of  $\sim 2 \mu\text{m}/\text{h}$ . The typical HgCdTe layer thicknesses used in these experiments were between 8  $\mu\text{m}$  and 10  $\mu\text{m}$ . The majority of the Hg $_{1-x}$ Cd $_x$ Te layers had an  $x$  value of  $\sim 0.20$  (intended for LWIR application), but both  $x \approx 0.33$  (for MWIR) and  $x \approx 0.40$  (for SWIR) were also used for comparison.

Samples were cleaved into roughly 7 mm  $\times$  7 mm pieces and later were sealed in a quartz ampoule with 100–1000  $\mu\text{l}$  of mercury under a vacuum of  $\sim 10^{-5}$  Torr. The samples were then placed in the center zone of a Lindburg 6 in.-diameter three-zone

furnace, which was held at 100°C. Samples were then heated to 250°C. Once the temperature had stabilized (approximately 5 min), the cycle annealing process was initiated. The first step of this process was to heat the samples to the annealing temperature (400–500°C), which was a variable in this study. Generally, this heating time took 2–3 min. The furnace was held at the annealing temperature for another 5 min before being brought back to 250°C. The cooling time from the annealing temperature to 250°C took 10–20 min, depending on the annealing temperature. This cycle was repeated. After the final cycle, the ampoule was held at 250°C before being removed and quenched in a water bath. A schematic of a typical cycle annealing experiment is shown in Fig. 1.

We measured the threading dislocation density using a dislocation decoration etch. This etching process consisted of a quick (2–3 s) 0.5% bromine-methanol etch to clean the surface, followed by a 35 s CrO<sub>3</sub>/HCl/H<sub>2</sub>O etch, and then another quick bromine-methanol etch to enhance the pit's visibility. The EPD was then counted with an optical Nomarski microscope.

We also recorded the x-ray rocking curves on selective samples using a PANalytical X'Pert Pro materials research diffractometer (MRD) on the (422) crystal plane to determine the full width at half maximum (FWHM), which gives a general assessment of the crystal quality. All measurements were taken with the Cu K $\alpha$  wavelength and were performed at room temperature.

## RESULTS AND DISCUSSION

Since we performed the annealing experiments well above the HgCdTe growth temperature, it was necessary for us to investigate the amount of Hg needed to maintain the surface morphology of the samples. If insufficient Hg was placed in the ampoule, the surface roughened significantly, as shown in Fig. 2. Calculated Hg pressures of approximately 7 atm, 25 atm, and 35 atm were needed to

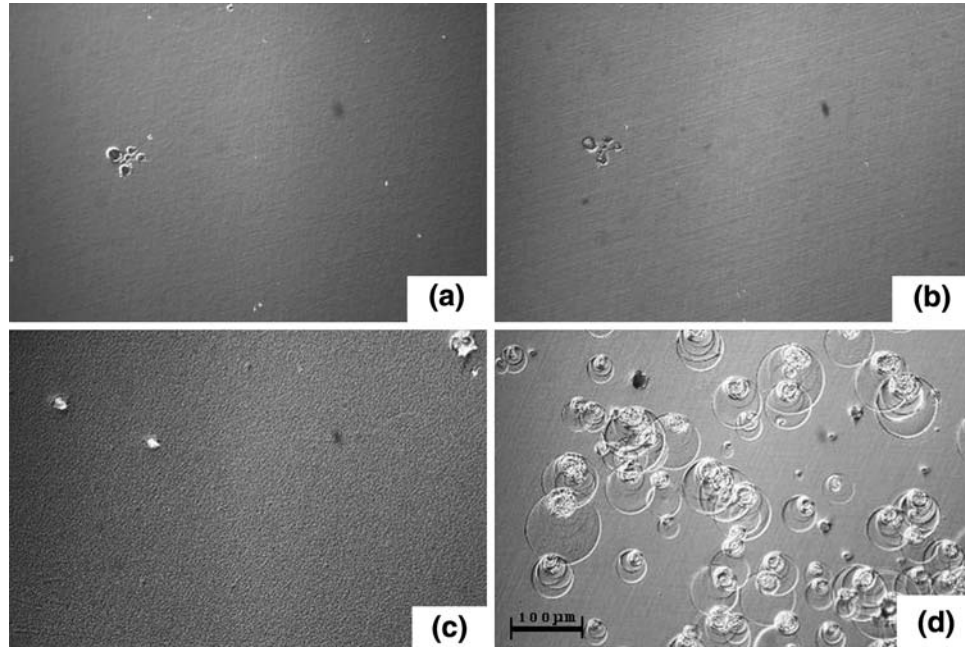


Fig. 2. Surface morphology of HgCdTe/Si samples. (a) As-grown, (b) TCA with correct amount of Hg, (c) TCA with insufficient amount of Hg, and (d) TCA with excessive amount of Hg.

preserve the surface for annealing temperatures of 400°C, 450°C, and 500°C, respectively. For anneals performed at 550°C, the HgCdTe surface morphology could not be preserved, regardless of the amount of Hg used. At all annealing temperatures, there was a problem with Hg condensation on the samples, as shown in Fig. 2d, when an excessive amount of Hg (>10 atm above the required Hg pressure) was used. Condensation could be partially prevented by our placing the sample face down, either directly on the inside bottom surface of the quartz ampoule or onto a clean piece of silicon. These techniques did not have a detrimental effect on the EPD. However, placing the samples face down on the ampoule's inner surface typically resulted in damage to the edges where the HgCdTe layer was in contact with the quartz. We found that putting the sample surface on a piece of silicon, leaving no HgCdTe surface exposed, prevented Hg condensation during cool down and did not show the edge damaging effects that occurred when the sample was placed directly on the ampoule's inner surface. Consequently, we obtained reproducible and better surface morphologies when the samples were placed face down on a piece of silicon. By using proximity annealing techniques, we could anneal the samples at higher temperatures, and the surface could be preserved for characterization, as shown in Fig. 2b.

The main focus of the remainder of the study was to explore the effects of various annealing parameters on the resulting EPD. We examined EPD as a function of annealing temperature for 400°C, 450°C, and 500°C, using four annealing cycles. Experiments at each temperature were repeated several times on

different samples. Table I shows the summary of the results for the three annealing temperatures, using samples with an as-grown layer EPD of  $6 \times 10^6 \text{ cm}^{-2}$  to  $1 \times 10^7 \text{ cm}^{-2}$ . The results of Table I show that the annealing temperature (for the range we studied) had little role in the reduction of EPD in the samples. While there is evidence to suggest that high temperatures might provide more consistent EPD results, the large amounts of Hg used at high temperatures, to maintain a good surface morphology, could create Hg condensation issues.

Figure 3 shows the variation of EPD as a function of the number of annealing cycles. To limit the Hg condensation, which could be a compounding problem for a larger number of annealing cycles, we performed these anneals at 400°C. As shown in Table I, the results for 400°C closely matched those at higher annealing temperatures. Figure 3 shows an initial exponential decay followed by a saturation of the EPD at  $\sim 1 \times 10^6 \text{ cm}^{-2}$  after four cycles. This finding differs from the results by Shin et al.,<sup>8</sup> who saw a further reduction of EPD in HgCdTe/GaAs for eight-cycle annealing as compared to four-cycle annealing. Likely, this difference resulted because the mismatch of the thermal coefficient of expansion and/or the lattice mismatch were much greater for the HgCdTe/Si system than for the HgCdTe/GaAs system. The larger mismatches in the case of HgCdTe/Si when compared with the HgCdTe/GaAs system were expected to play a role in the higher saturation in the EPD value. We measured the EPD values in the  $8 \times 10^5 \text{ cm}^{-2}$  to  $9 \times 10^5 \text{ cm}^{-2}$  range for some samples, but the overall EPD saturated at  $\sim 1 \times 10^6 \text{ cm}^{-2}$ .

**Table I. Etch pit density after four-cycle annealing at different temperatures**

Temperature (°C)	Average EPD (cm <sup>-2</sup> )	Standard Deviation (cm <sup>-2</sup> )
400	$1.2 \times 10^6$	$5.2 \times 10^5$
450	$1.6 \times 10^6$	$7.2 \times 10^5$
500	$1.4 \times 10^6$	$3.2 \times 10^5$

The as-grown EPD of the samples used for this set of experiments was in the range  $6 \times 10^6$  cm<sup>-2</sup> to  $1 \times 10^7$  cm<sup>-2</sup>.

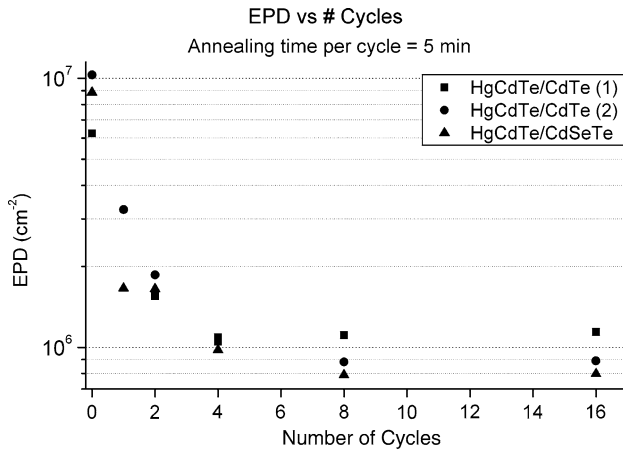


Fig. 3. Variation of EPD with the number of annealing cycles for an annealing time of 5 min per cycle and an annealing temperature of 400°C.

To ensure that the EPD reduction was, indeed, directly related to the number of annealing cycles rather than to the total duration of annealing time, we also conducted experiments where the total annealing time was held constant but the number of cycles was varied. We performed single through four-cycle anneals, while keeping the total annealing time constant at 20 min. Specifically, we held a single-cycle anneal at 400°C for 20 min, a two-cycle anneal for 10 min each cycle, a three-cycle anneal for 7 min each cycle, and a four-cycle anneal for 5 min each cycle. These results are shown in Fig. 4. From the data presented in Figs. 3 and 4, it is clear that the total annealing time was not causing the EPD reduction, but rather the effect was caused by the cyclical nature of the annealing. Additional experimentation of four-cycle annealings with 10-min and 20-min duration for each cycle yielded no advantage over our using 5-min cycles.

Figure 5 shows typical x-ray rocking curves recorded on as-grown and 16-cycle annealed (at 400°C) HgCdTe/Si samples. The crystalline quality has clearly improved, with a reduction in the FWHM from 120 arcsec to 62 arcsec. This result is consistent with those of other studies that show a correlation between x-ray FWHM and defect density.<sup>11</sup> The variation of FWHM with the number

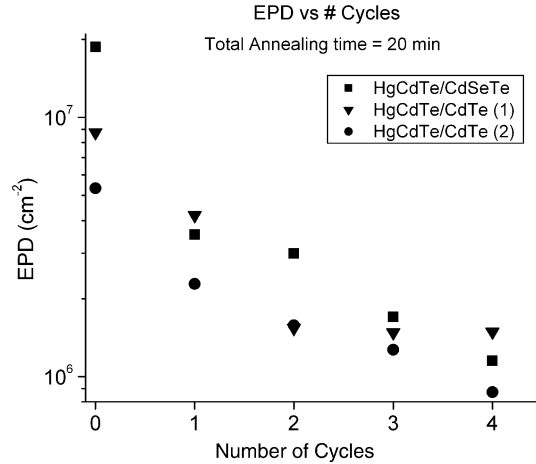


Fig. 4. Variation of EPD with number of annealing cycles, with the total annealing time being kept constant at 20 min for an annealing temperature of 400°C.

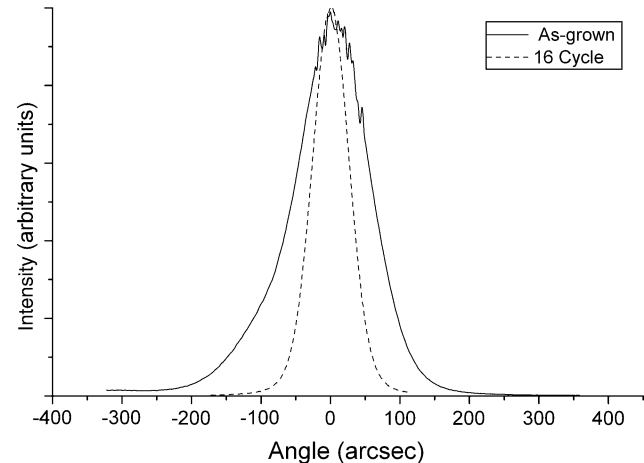


Fig. 5. Comparison between the rocking curves recorded on an as-grown sample having an EPD of  $1 \times 10^7$  cm<sup>-2</sup> (solid line) and a 400°C and a 16-cycle annealed sample having an EPD of  $8.9 \times 10^5$  cm<sup>-2</sup> (broken line). The FWHM values for the as-grown and the annealed samples are 120 arcsec and 62 arcsec, respectively.

of annealing cycles is shown in Fig. 6. The x-ray measurements were performed prior to our performing the EPD etch. Figure 6 also shows an initial exponential decay in FWHM of the x-ray rocking curves as the number of annealing cycles increases, as observed previously in Fig. 3 for EPD as a function of the number of annealing cycles. However, unlike the values of the EPD versus number of annealing cycles in Fig. 3, the values of the x-ray rocking curve FWHM slowly continue to decrease as the number of annealing cycles increases. This result might indicate that the overall quality of the crystal would continue to improve as the number of annealing cycles increases, but at a smaller rate than can be discerned using a defect decoration etch.

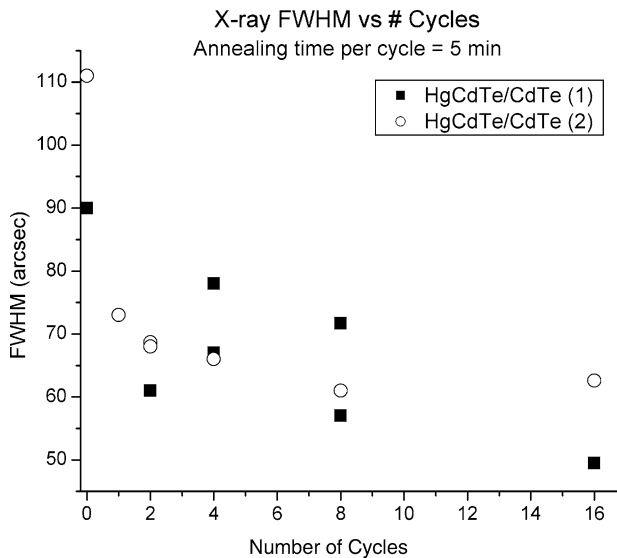


Fig. 6. Variation of x-ray rocking curve FWHM of the (422) crystal plane with number of annealing cycles.

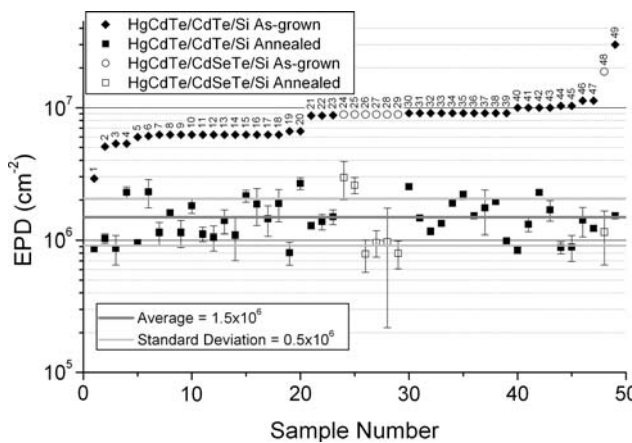


Fig. 7. Depiction of our comprehensive TCA experimental data. For each sample, EPD values before and after TCA are shown.

To understand the  $1 \times 10^6 \text{ cm}^{-2}$  EPD saturation, we used for the TCA experiments HgCdTe/Si samples with a large variation in as-grown EPD. As stated previously, the results of experiments with variable annealing temperatures indicated that the annealing temperature was not the leading factor in EPD reduction. As a result, the majority of further anneals were carried out at  $400^\circ\text{C}$ , although some  $450^\circ\text{C}$  and  $500^\circ\text{C}$  anneals were also preformed for comparison. The results of this comprehensive annealing study are shown in Fig. 7. The as-grown EPD of the sample had little to no effect on the post-annealed EPD value measured within the as-grown EPD range investigated. The post-anneal EPD of all samples in Fig. 7 had an average value of  $1.5 \times 10^6 \text{ cm}^{-2}$ , with a standard deviation of  $0.5 \times 10^6 \text{ cm}^{-2}$ . This result differs from that in the work done by Arias et al.,<sup>12</sup> where a correlation between as-grown EPD and post-annealed EPD was observed. This

difference could be due to the absence of multiple annealing cycles employed in their study; hence, their samples did not reach their final EPD saturation points.

While the variation in as-grown HgCdTe EPD ranged from  $3 \times 10^6 \text{ cm}^{-2}$  to  $3 \times 10^7 \text{ cm}^{-2}$ , the variation in the as-grown CdTe buffer layer EPD was rather large, ranging from  $2.5 \times 10^5 \text{ cm}^{-2}$  to  $3 \times 10^7 \text{ cm}^{-2}$ , as measured using the Everson etch<sup>13</sup> (not shown in Fig. 7). The EPD of a typical as-grown HgCdTe layer showed little correlation with the EPD of the as-grown CdTe buffer layer, except when the as-grown CdTe EPD was greater than mid- $10^6 \text{ cm}^{-2}$ , at which point the minimum as-grown HgCdTe EPD began to mimic the as-grown CdTe EPD. In spite of two orders of magnitude variation in the as-grown CdTe buffer layer EPD, after TCA, there was no correlation between the final HgCdTe EPD and the as-grown CdTe buffer layer EPD. As seen in Fig. 7, the results of samples such as sample no. 23, with an as-grown CdTe EPD of  $1.2 \times 10^7 \text{ cm}^{-2}$  (not shown), showed an HgCdTe EPD reduction to the same range as that of other samples [such as 21, 22, 46, and 47, which have an as-grown CdTe buffer layer EPD of  $4.6 \times 10^5 \text{ cm}^{-2}$  (not shown), and samples 7 through 18, which have an as-grown CdTe buffer layer EPD of  $1.1 \times 10^6 \text{ cm}^{-2}$  (not shown)]. At this time, it is not clear what effect the TCA has on the buffer layer EPD. Based on the results of our study, it appears that the dislocation reduction by TCA occurs regardless of the origin of the dislocations, whether they nucleate from the CdTe/Si or the HgCdTe/CdTe interface.

In an effort to explore further the effect of the CdTe buffer layer on the HgCdTe EPD, we compared the results of TCA treatment on HgCdTe/CdTe/Si samples with those on HgCdTe/CdSeTe/Si samples, where a lattice-matched CdSeTe buffer layer was used instead of CdTe. The results on these layers are presented in Figs. 3 and 4. In total, five HgCdTe samples with a CdSeTe/Si composite substrate were annealed for four or more cycles and are represented by empty circles in Fig. 7. Though the samples numbered 24 through 29 in Fig. 7 exhibited some of the lowest EPDs of all the samples, the average of these five samples was  $1.5 \times 10^6 \text{ cm}^{-2}$ , with a deviation of  $1 \times 10^6 \text{ cm}^{-2}$ . In Fig. 3, the samples with a CdSeTe buffer layer show a trend of reduction and saturation in EPD, with respect to the number of annealing cycles, similar to that of the samples with the CdTe buffer layer. The majority of the  $\text{Hg}_{1-x}\text{Cd}_x\text{Te}$  layers used in this experiment had  $x \approx 0.20$ , but layers with  $x \approx 0.33$  and  $x \approx 0.40$  were also included in our experiments. Although this was not an exhaustive study, we did not find a correlation between EPD and Cd composition.

The HgCdTe layers grown on bulk CdZnTe samples, which were subjected to annealing conditions similar to those for the HgCdTe layers grown

on the composite substrates, showed a half to one order of magnitude reduction in EPD, from  $5 \times 10^5 \text{ cm}^{-2}$  to values as low as  $5-10 \times 10^4 \text{ cm}^{-2}$ . Clearly, the pinning in EPD observed in HgCdTe/Si after TCA is not an intrinsic property of the HgCdTe crystal but is related to the substrate on which it is grown. As with the HgCdTe/Si, the HgCdTe grown on bulk CdZnTe samples showed little to no correlation between the annealing temperature and the resulting EPD. The HgCdTe on bulk CdZnTe also exhibited EPD saturation after undergoing four annealing cycles as in the case of HgCdTe/Si.

## CONCLUSIONS

Thermal cycle annealing using temperatures  $\geq 400^\circ\text{C}$  has been shown to reduce effectively and reproducibly the EPD of HgCdTe/CdTe/Si samples to  $1 \times 10^6 \text{ cm}^{-2}$ . Experimental evidence using a lattice-matched CdSeTe buffer layer on silicon gave evidence that the pinned value is substrate related and not due to an intrinsic property of HgCdTe itself or a product of its growth conditions. The reports by others that have identified a defect reduction down to  $\sim 5 \times 10^5 \text{ cm}^{-2}$  in HgCdTe/GaAs is consistent with this hypothesis.<sup>8,9,12</sup> The fact that defect reduction can still be seen when bulk CdZnTe substrates are utilized shows that the defect reduction trend continues as the substrate material becomes more closely lattice matched with HgCdTe. The consistency of minimum dislocation density after TCA across different sets of experiments suggests that there is not a specific annealing parameter that can be tweaked to achieve an EPD lower than  $\sim 1 \times 10^6 \text{ cm}^{-2}$  for the HgCdTe/CdTe/Si system. Among several parameters studied in this work, the number of annealing cycles had the greatest influence on decreasing the defect density, but this effectiveness drastically diminished after four annealing cycles.

## ACKNOWLEDGEMENTS

The work at George Mason University (GMU) is supported by the Army Research Office (ARO) under grant no. W911NF-07-2-0055 and also by the Penn State Electro-Optics Center.

## REFERENCES

1. N.K. Dhar, M. Zandian, J.G. Pasko, J.M. Arias, and J.H. Dinan, *Appl. Phys. Lett.* 70, 1730 (1997).
2. P.S. Wijewarnasuriya, M. Zandian, D.D. Edwall, W.V. McLevige, C.A. Chen, J.G. Pasko, G. Hildebrandt, A.C. Chen, J.M. Arias, A.I. D'Souza, S. Rujirawat, and S. Sivananthan, *J. Electron. Mater.* 27, 546 (1998).
3. T.J. de Lyon, R.D. Rajavel, J.A. Vigil, J.E. Jensen, O.K. Wu, C.A. Cockrum, S.M. Johnson, G.M. Venzor, S.L. Bailey, I. Kasai, W.L. Ahlgren, and M.S. Smith, *J. Electron. Mater.* 27, 550 (1998).
4. T. Parodos, E.A. Fitzgerald, A. Caster, S. Tobin, J. Marciniec, J. Welsch, A. Hairston, P. Lamarre, J. Riendeau, B. Woodward, S. Hu, M. Reine, and P. Lovecchio, *J. Electron. Mater.* 36, 1068 (2007).
5. S.H. Shin, J.M. Arias, M. Zandian, J.G. Pasko, and R.R. DeWames, *Appl. Phys. Lett.* 59, 2718 (1991).
6. Y. Chen, S. Farrell, G. Brill, P. Wijewarnasuriya, and N. Dhar, *J. Cryst. Growth* 310, 5303 (2008).
7. L. He, S.L. Wang, J.R. Yang, M.F. Yu, Y. Wu, X.Q. Chen, W.Z. Fang, Y.M. Qiao, Y. Gui, and J. Chu, *J. Cryst. Growth* 201-202, 524 (1999).
8. S.H. Shin, J.M. Arias, D.D. Edwall, M. Zandian, J.G. Pasko, and R.R. DeWames, *J. Vac. Sci. Technol. B* 10, 1492 (1992).
9. T. Sasaki and N. Oda, *J. Appl. Phys.* 78, 3121 (1995).
10. Y. Chen, G. Brill, and N. Dhar, *J. Cryst. Growth* 252, 270 (2003).
11. J.D. Benson, R.N. Jacobs, J.K. Markunas, M. Jaime-Vasquez, P.J. Smith, L.A. Almeida, M. Martinka, M.F. Vilela, and U. Lee, *J. Electron. Mater.* 37, 1231 (2008).
12. J.M. Arias, M. Zandian, S.H. Shin, W.V. McLevige, J.G. Pasko, and R.R. DeWames, *J. Vac. Sci. Technol. B* 9, 1646 (1991).
13. W.J. Everson, C.K. Ard, J.L. Sepich, B.E. Dean, G.T. Neugebauer, and H.F. Schaake, *J. Electron. Mater.* 24, 505 (1995).